

Modified Spin-Wave Theory for Nanomagnets : Application to the Keplerate Molecule $\text{Mo}_{72}\text{Fe}_{30}$

Olivier CÉPAS^{*)} and Timothy ZIMAN^{**)}

Institut Laue Langevin, B.P. 156, 38042 Grenoble, France.

We adapt Takahashi's modified spin-wave theory to the context of nano-magnets, and apply it to the molecular compound based on the giant magnetic molecule $\text{Mo}_{72}\text{Fe}_{30}$. This involves solving numerically the mean-field equations and then forcing the sublattice magnetizations to zero by means of local chemical potentials for the magnons. We have thus constructed a quantum state with no local magnetization at all temperatures, appropriate to a finite-size system, but with strong correlations. We compare theoretical results to specific heat and ESR measurements.

§1. Introduction

Much effort has been devoted to low-dimensional antiferromagnetism in the past years and difficult questions as to whether a magnetic system of given geometry and spin-symmetry displays long-range order or remains disordered at zero temperature were tackled. For instance, for two dimensional isotropic Heisenberg models the triangular lattice or the $J_1 - J_2$ square model were studied by a variety of analytical and numerical techniques in order to establish order at low temperature.¹⁾ These techniques include finite-size scaling, i.e. extrapolation from finite systems for which exact numerical results are available to the thermodynamic limit of physical interest. In the newer field of nano-magnetism the question is rather inverted: as these systems are finite, by definition there is no long range order. Because of thermodynamic or quantum fluctuations it is not possible to break spontaneously any symmetry. For large nanomolecules, there should be traces of incipient long range order essentially in the low frequency parts of the spectrum. The issue, then, is rather to find an accurate description of the system and of its dynamics.

Several antiferromagnetic nano-magnets have been studied recently, ranging from small isolated molecular units, such as V_3 to the giant molecule $\text{Mo}_{72}\text{Fe}_{30}$,²⁾ via a large number of intermediate-size clusters. As for potential applications, they are promising materials if their magnetic states can be externally "read", for example by using a spin-polarized current as proposed in multilayers.³⁾ From a fundamental point of view, they are interesting systems to study the crossover from simple quantum molecular systems to larger systems that may behave as classical Néel states. They can, to a first approximation, be treated as isotropic. According to the original picture by Anderson for systems of continuously degenerate broken symmetries,⁴⁾ a manifold of degenerate classical Néel states is obtained when a family of finite energy states (the "tower" of states) of the system of size N collapse onto the ground state

^{*)} E-mail address: cepas@ill.fr

^{**) Also at the CNRS, LPM2C, UMR 5493, Grenoble}

when $N \rightarrow +\infty$ (as $1/N$). Systems with frustration are particularly interesting in that it may amplify the competition between quantum-mechanically disordered and Néel-like states. There is even no guarantee that the system would order in the thermodynamic limit. It is also known that competitions arise when an external magnetic field is applied to systems such as the infinite triangular lattice⁵⁾ or the Kagomé lattice.⁶⁾ Nano-magnets are similarly being studied under field.⁷⁾ An external magnetic-field also allows for measurements of crossing of excited states and quantized magnetization processes.⁸⁾

$\text{Mo}_{72}\text{Fe}_{30}$ is an abbreviation for a recently synthesized giant molecule that consists of 30 Fe^{3+} $S = 5/2$ ions which occupy the vertices of an icosidodecahedron (known as one of the Kepler solids, hence the name Keplerate for the molecule).²⁾ Experiments show an absence of magnetic order at low temperatures, suggesting that the molecules of the solid are relatively isolated from one another.²⁾ This molecule is highly frustrated, consisting of triangle- and pentagon-sharing vertices. Thus the spins of each nano-molecular unit may be seen as forming a finite closed surface. When a magnetic-field is applied, there is a dip in the magnetization as function of field at $1/3$ of the saturation field, which has been interpreted as proximity to the $\uparrow\uparrow\downarrow$ state.⁷⁾ There are also predicted features such as a large jump in the magnetization just before saturation,⁹⁾ reminiscent of the divergent susceptibility in bulk systems.¹⁰⁾

From the theoretical standpoint, studies assuming classical interacting spins have been made. Axenovich and Luban¹¹⁾ argued that such a lattice could sustain the same order as the triangular lattice (sublattice spins forming 120° angles) at zero temperature, thanks to the possibility of decomposing the icosidodecahedron into three sublattices. By construction, such a classical state breaks time-reversal symmetry, although this is forbidden in a finite-size system. More recently classical Monte-Carlo calculations have been performed at finite temperatures.¹²⁾ As expected, the thermal fluctuations prevent the system from ordering, but also give a large specific heat at low temperatures. From a purely classical point of view, it is difficult to explain simultaneously the absence of magnetic-order and a vanishing specific heat (as observed¹³⁾), because the modes that destroy the magnetic order would contribute to the specific heat by $k_B/2$ per mode. Quantum fluctuations have not been considered so far and should be able to resolve such issues. Schnack et al. have discussed a simplified quantum model where all the spins of a given sublattice are connected to all the spins of the other sublattices.¹⁴⁾ Such a model is integrable and they find rotational bands as low-lying excitations,¹⁴⁾ the first band being confirmed by a DMRG in a more realistic Heisenberg system with nearest neighbor interactions only.¹⁵⁾ There is no theory, however, that bridges the gap between purely classical approaches, such as that of Ref.^{11), 12)} and quantum ones.

Recently, Nojiri et al. have observed optical resonances at low temperatures.¹³⁾ They have interpreted these resonances as transitions from the ground state to the first excited state. In a purely *spin-isotropic* model, such as in Ref.,¹⁴⁾ the transition probability vanishes because of the conservation of the total spin. To explain such transitions, one needs to invoke the presence of anisotropic interactions, whether the transitions be of magnetic origin as, possibly, in low-dimensional spin-liquids¹⁶⁾ or of

electric origin, which could proceed via an anisotropic coupling with the phonons.¹⁷⁾ It seems therefore important to consider what the possible additional couplings to a Heisenberg Hamiltonian are and whether these corrections are able to capture the optical processes that have been observed. Hasegawa and Shiba have considered several anisotropic corrections to their classical Hamiltonian¹²⁾ : the dipole-dipole interactions could be safely neglected thanks to large Fe-Fe distances, the first corrections being single-ion, or, possibly, of Dzyaloshinskii-Moriya type. We have considered below the simplest single-ion anisotropy which is allowed in $S = 5/2$ systems and often dominates the anisotropic interactions.

Such a model lacks the simplicity of that of Ref.¹⁴⁾ and can not be treated exactly. As previously noticed, the size of the Hilbert space, $6^{30} \sim 10^{23}$, prevents using techniques such as exact numerical diagonalisations. We have adopted a different approach by solving the mean-field problem (which is classical in essence) first and introducing the quantum corrections by means of Holstein-Primakoff bosons. Doing so, we artificially break the symmetry by allowing the magnetic order to occur. To restore the symmetry, we use a technique that has been introduced by Takahashi.^{18),19)} It consists of enforcing *a posteriori* the magnetizations to be zero on each site. This allows one to find phases with no sublattice magnetization, i.e. which do not break the time-reversal symmetry.

In section §2, we solve numerically the mean-field equations for quantum spins on an icosidodecahedron and find in particular a form of magnetic order at zero temperature which is close to, but not exactly the same as, the 120° structure of the triangular lattice. In section §3, we calculate the first quantum corrections and apply Takahashi's method to enforce the local constraints. We discuss the excitation spectrum, the two-point correlation functions in the ground state and some observables such as the ESR intensity or the specific heat at zero-field.

§2. Mean-Field Theory of the Models with Anisotropy

Since the molecules are relatively isolated from one another, we consider a one-molecule problem, i.e. a spin model where the spins occupy the vertices of an icosidodecahedron (Fig. 1)

$$H = \frac{1}{2} \sum_{\langle i,j \rangle} J \mathbf{S}_i \cdot \mathbf{S}_j + \sum_{i=1}^N D^{(i)} (S_i^{(i)})^2, \quad (2.1)$$

where \mathbf{S}_i is a quantum spin operator of $S = 5/2$ (of Fe^{3+}), J is the antiferromagnetic coupling between the nearest neighbors $\langle i,j \rangle$. The factor $1/2$ removes double counting. $N = 30$ is the number of sites. We consider two types of anisotropy :

1. $D^{(i)}$ are *global* single-ion anisotropies, with the axis identical for all sites. This is not very realistic given the geometry of the icosidodecahedron, but is a simple model to compare with.
2. $D^{(i)}$ are *local* single-ion anisotropies, and (i) is a local direction which points towards the center of the solid at each site, $D^i = D \hat{\mathbf{R}}_i$, where $\hat{\mathbf{R}}_i$ is the position vector of site i , as in Ref.¹²⁾

In both cases, the strength of the anisotropy is small $|D|/J = 0.1$, which is justified by the fact that Fe^{3+} has a closed shell ($L_{\text{tot}}=0$). We consider easy-plane or easy-axis types. In the Zeeman coupling, we take $g = 2$. At $T = 0$, one wants to minimize the energy (2.1). This is done by iterating numerically the $3N$ self-consistent mean-field equations for quantum spins, starting from random initial states (up to 10^4).

For model 1 with easy-plane anisotropy, the system converges to a simple three-sublattice 120° magnetic order at zero temperature (Fig. 1, left). This is the state found in Ref.¹¹⁾ except that the present anisotropy forces the spins to lie in a plane perpendicular to the D-vector. The energy per spin is simply $E_0/N = -S^2$. We note that replacing S^2 by $S(S + 1)$ ^{11),20)} does not give a correct estimation of the zero-point energy. For this a calculation of the quantum corrections has to be performed (see below) and generally gives different results.

For model 2, the state is very close to the 120° order except that it is more *tangential* to the sphere (Fig. 1, right). To see it more clearly, we have depicted the distribution of classical scalar products $\langle \mathbf{S}_i \cdot \mathbf{S}_j \rangle = \langle \mathbf{S}_i \rangle \cdot \langle \mathbf{S}_j \rangle$ in fig. 5. The majority of nearest neighbor bonds have a scalar product close to $-1/2$, corresponding to an angle of 120° , but some of them depart from that angle. The energy is $E_0/N = -0.989S^2$ for $D/J = 0.1$. It is interesting to note that the state accommodates fairly well the local single-ion anisotropy: the energy increase is a tenth of the anisotropy. We have found a large number of degenerate states, probably owing to the large number of symmetries of the icosidodecahedron.

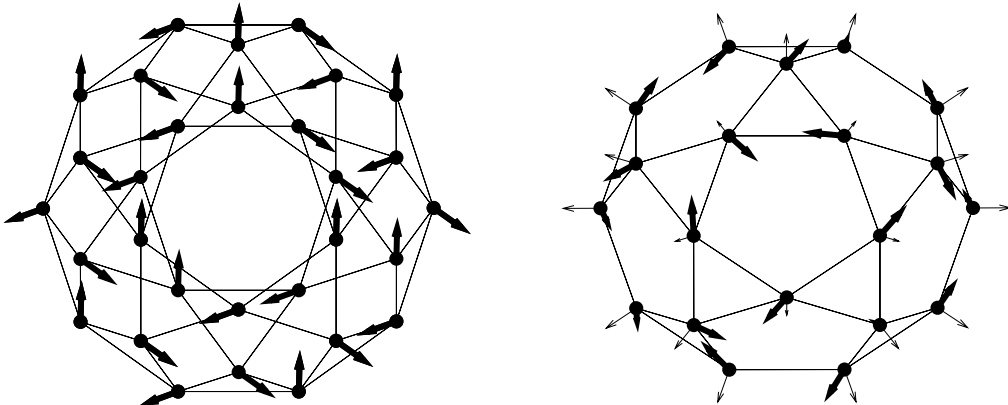


Fig. 1. Spin arrangements on the icosidodecahedron lattice (thick vectors), calculated by mean-field theory at $T = 0$ and zero external field. Left : A *global* easy-plane anisotropy identical for all spins and perpendicular to the plane of the sheet favors a 3-sublattice *coplanar* 120° state identical to that of Ref.¹¹⁾ There is a continuous degeneracy as it is possible to rotate the spin of one sublattice in the plane. Right: The easy-plane $D^{(i)}$ vectors (represented by thin vectors) are *local* and point towards the center of the solid at each point. The spin order is more *tangential* to the sphere. The degeneracy is quite large.

§3. Holstein-Primakoff Modes in Finite-Size Systems

3.1. Method

Having solved the mean-field problem in the previous section, we can introduce the first quantum corrections by expanding the free-energy about a mean-field state. To do this, we work in a new frame where the new local coordinate axis at site i , called z' , coincides with the classical direction of the spin on the same site,²¹⁾ given by the solution of the mean-field problem. We then use the Holstein-Primakoff representation of the spins in terms of boson operators *in the new frame*:

$$S_i^{+'} = \sqrt{2S - a_i^\dagger a_i} a_i; \quad S_i^{-'} = a_i^\dagger \sqrt{2S - a_i^\dagger a_i}; \quad S_i^{z'} = S - a_i^\dagger a_i \quad (3.1)$$

where the primes correspond to the new local axis. By expanding the Hamiltonian to second-order in the operators a_i, a_i^\dagger ,^{*)} it takes the form of free bosons in *real* space:

$$H = E_0 + \frac{E_0}{S} + \frac{1}{2} \sum_{\langle i,j \rangle} \left(A_{ij} a_i^\dagger a_j + A_{ij}^* a_i a_j^\dagger + B_{ij} a_i^\dagger a_j^\dagger + B_{ij}^* a_i a_j \right) \quad (3.2)$$

E_0 is the mean-field energy that we found in the previous paragraph. The coefficients A_{ij} and B_{ij} ($\mathcal{O}(S)$) are function of the couplings and the local rotation matrices.²¹⁾ The Hamiltonian is Hermitian and we have $A_{ij} = A_{ji}^*$ and $B_{ij} = B_{ji}$. To define the fourth term of (3.2), we had to commute the $a_j^\dagger a_j$ operators. It gives a constant term that reduces to the second term of eq. (3.2), E_0/S . Such a Hamiltonian is usually diagonalized by a Bogoliubov transformation which ensures the bosonic characters of the final bosons.^{21), 22)} Such a transformation can generally be constructed numerically in systems with a sufficient amount of anisotropy,^{23), 24)} but not directly when a continuous symmetry leads to the existence of Goldstone modes. In this case the bosonization procedure is singular, and it is well-known for the infinite triangular lattice that the Hamiltonian can not be bosonized at $k = 0$ or $k = \pm 4\pi/3$.^{25), 26)} The singular Goldstone modes can easily be separated out for infinite systems, simply by omitting the $k = 0, \pm 4\pi/3$ modes in the sums over k ,^{25), 26)} but here there is no k -space. In any case, in a finite-size system, the Goldstone modes are spurious since the assumption of a broken-symmetry phase is obviously incorrect. Takahashi^{18), 19)} and Hirsch and Tang²⁷⁾ have tackled this problem and imposed the condition that the magnetization should be zero in a finite-size system,

$$\langle S_i^{z'} \rangle = S - \langle a_i^\dagger a_i \rangle = 0, \quad (3.3)$$

for all sites i . This is reminiscent of the paper by Rastelli and Tassi who introduced this idea for the paramagnetic phase of a ferromagnet.²⁸⁾ If in special cases, the condition could be enforced by a unique Lagrange multiplier,^{19), 27)} the N local constraints usually oblige us to introduce N different Lagrange multipliers

^{*)} Strictly speaking it is a simplified version of Takahashi's method (see below) who, for the simpler square lattice model, used the Dyson-Maleev representation and took into account the interaction between the spin-waves at the Hartree-Fock level.

$\{\lambda_i\}, i = 1, \dots, N$:

$$H' = H + \sum_{i=1}^N \lambda_i a_i^\dagger a_i \quad (3.4)$$

The $\{\lambda_i\}$ can also be viewed as *local* chemical potentials for spin-flips, since $a_i^\dagger a_i$ is the number operator of spin-flips on site i . To include these additional terms, the Hamiltonian in eq. (3.2) is modified by simply replacing A_{ij} by $A'_{ij} = A_{ij} + \lambda_i \delta_{ij}$ and adding a constant term to the energy, $-\frac{1}{2} \sum_i \lambda_i$. Now all the quantities, and the excitation spectrum in particular, will depend upon the $\{\lambda_i\}$. We shall determine the set of $\{\lambda_i\}$ by solving the N equations (3.3). To do this we have to diagonalize the Hamiltonian H' and then calculate the expectation values in the ground state, such as $\langle a_i^\dagger a_i \rangle$. When finite Lagrange multipliers are added, the Goldstone modes are removed from the problem and it is possible to construct numerically a Bogoliubov transformation. The diagonalized Hamiltonian then takes the form:

$$H' = E_0 + \frac{E_0}{S} + \sum_{j=1}^N \omega_j \left(a_{\omega_j}^\dagger a_{\omega_j} + \frac{1}{2} \right) - \frac{1}{2} \sum_{j=1}^N \lambda_j \quad (3.5)$$

where $a_{\omega_j}^\dagger$ is a boson operator that creates an excitation of energy ω_j . Note that the zero-point energy is given by $E_0/S + \frac{1}{2} \sum_j (\omega_j - \lambda_j)$ (the two terms cancel out for a simple easy-axis ferromagnet for instance). The Bogoliubov transformation also gives the eigen-operators as function of the local boson operators and all the expectation values of the form $\langle a_i^\dagger a_j \rangle$, for instance, can be calculated. We then solve the eqs. (3.3) by a standard numerical routine that finds the roots of a set of non-linear equations. Once the Lagrange multipliers are found, the state satisfies $\langle \mathbf{S}_i \rangle = 0$. We then compute various physical quantities, such as the excitation spectrum ω_j , and the total energy $E(T)$. The latter needs the explicit determination of the Lagrange multipliers at each temperature and needs subtraction of the magnon chemical potential part. We also compute the two-point correlation functions $\langle \mathbf{S}_i \cdot \mathbf{S}_j \rangle$ of the ground state. The solution is only valid at low temperatures because the approach starts from a low-temperature minimum that is obviously different from the paramagnetic state. We expect the present solution to depart from the exact solution when $T \sim T_N$ (where T_N is the mean-field Néel temperature of the classical system).

3.2. Simplified Model with Global Anisotropy Axis

We first start by giving the results of a simpler problem where all the D -vectors are parallel to the same axis (model 1). In this case, mean-field theory predicts a simple coplanar state with three sublattices of spins at 120° (Fig. 1, left). Purely classical models were similarly considered in Refs.^{11), 12)} and we would like to stress what changes quantum fluctuations bring to the classical picture. First of all, the state that we have constructed satisfies the constraint of zero magnetization on each site, as it should for a finite-size system. Nevertheless, there are strong correlations that reflect features of the original classical state. We shall now describe these.

Correlations. In Fig. 2, we compare the distribution of the scalar products $\langle \mathbf{S}_i \cdot \mathbf{S}_j \rangle$ on the different bonds for the mean-field solution and the Takahashi's method. As expected, the quantum fluctuations have broadened the distribution (Fig. 2, left). A question is whether or not fluctuations have destroyed the correlations between spins that are far away from each other. In other words, how does the correlation length compare with the size of the molecule? In Fig. 2, we look at pairs of spins at given distances. The nearest neighbors are still strongly correlated, but the correlation of far neighbors have decreased, although not to zero (Fig. 2, right).

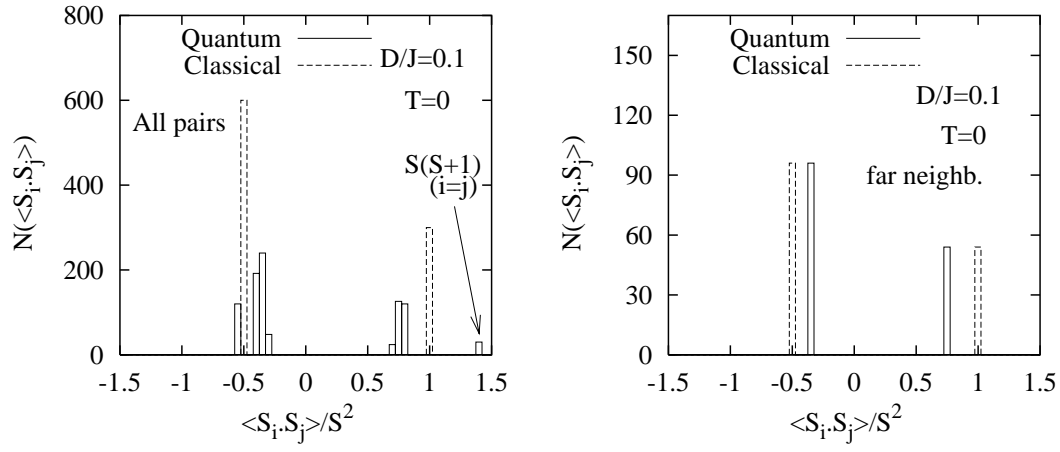


Fig. 2. Number of bonds with a given value of the correlation function for all the 900 bonds (left) and far neighbors (right). Global anisotropy axis. The quantum correlations $\langle \mathbf{S}_i \cdot \mathbf{S}_j \rangle$ are obtained by applying Takahashi's method whereas the classical correlations are simply given by $\langle \mathbf{S}_i \cdot \mathbf{S}_j \rangle = \langle \mathbf{S}_i \rangle \cdot \langle \mathbf{S}_j \rangle$. The classical ground state is a 3-sublattice coplanar state with 120° angles. On the right, we see that the quantum fluctuations reduce the correlations between far neighbors, though not to zero.

Specific Heat. The classical specific heat, computed by Monte-Carlo simulation, remains finite at zero temperature and shows a peak at $0.3J$.¹²⁾ The specific heat calculated with quantum corrections exhibits different features (Fig. 3, right). It vanishes at zero temperature and the peak (which is fairly independent of the strength of the anisotropy) is pushed to higher temperatures $\sim 3J$, that is more consistent with experiment. We now compare the results of the modified spin-wave theory with that of a high-temperature expansion that is given at second order by the analytic expression, $E/NJ = -51.04J/T + 148.87(J/T)^2$. Note that it would be highly desirable to have higher-order terms, that can be obtained systematically.²⁹⁾ We plot the energies in Fig. 3, left. We see that there is clearly a regime at high temperature where the modified spin-wave theory breaks down. In this regime the specific heat is greatly over-estimated, and consequently the position of the peak may be over-estimated too. Nonetheless, at low temperatures, the quantum corrections should yield the correct behavior of the specific heat and provide a reliable way of comparing with experiments.

Excitation Spectrum and ESR intensities. We start with the fully-connected model introduced in Ref.¹⁴⁾ where all the spins of a given sublattice are connected

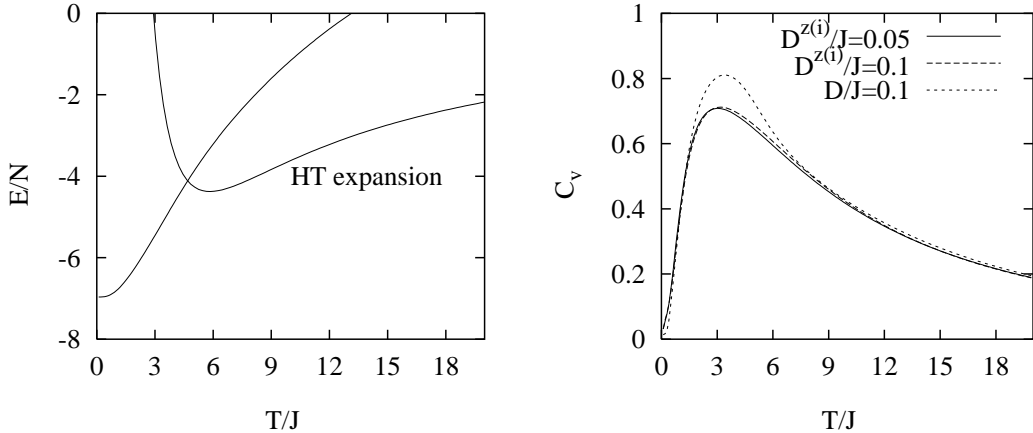


Fig. 3. Energy per spin vs. temperature, calculated by modified spin-wave theory and high-temperature (HT) expansion (left). There is a critical temperature above which the modified spin-wave theory breaks down. Specific heat vs. temperature for the system with global anisotropy, $D/J = 0.1$ (section 3.2) and local anisotropy, $D^i/J = 0.05$ and $D^i/J = 0.1$ (section 3.3). The present theory breaks down above $T \gtrsim 3J$ where the specific heat is overestimated. The last two curves are almost identical, thus indicating that C_v is insensitive to the strength of the anisotropy.

to all the spins of an other sublattice, $\frac{J}{5} (\tilde{\mathbf{S}}_A \cdot \tilde{\mathbf{S}}_B + \tilde{\mathbf{S}}_B \cdot \tilde{\mathbf{S}}_C + \tilde{\mathbf{S}}_C \cdot \tilde{\mathbf{S}}_A)$, where $\tilde{\mathbf{S}}_A$ is a super-spin obtained by adding $N/3$ spins S on sublattice A . The Hamiltonian factorizes and the energies are simply extracted from $\frac{J}{10} (\mathbf{S}^2 - (S_A^2 + S_B^2 + S_C^2))$ ($\mathbf{S} = \tilde{\mathbf{S}}_A + \tilde{\mathbf{S}}_B + \tilde{\mathbf{S}}_C$). The excited states form separated rotational bands with energies depending upon $S(S+1)$,^{14),30)} the lowest of which is constructed by combining the three $S_{A,B,C} = NS/3$ maximum spins. These lowest states are precisely the tower of states that were found in exact numerical diagonalization of the triangular lattice with nearest neighbor interactions.²⁶⁾ These states would collapse onto the classical ground state if the size of the system N were allowed to go to infinity.²⁶⁾ The ground state energy per spin is exactly $-6.5J$ and among all the states of the rotational bands there are three triplet states at $0.2J$ and six at $5.2J$.¹⁴⁾ By the approximate method of section 3.1, we have obtained a ground state energy of $-6.498J$ and three states at $0.11J$ and $0.08J$ (twice degenerate)*) and the others at $5.0J$, which is in overall good agreement (Fig. 4, left, $D^z/J = 0$).

We now consider the more realistic model (2.1) where the additional couplings J' introduced in the previous paragraph are reduced to zero. We see that the degenerate excited states at $5.0J$ are split when one reduces J' (Fig. 4, left). The final spectrum at $J' = 0$ is very different from that of $J' = J$ and the new gaps have nothing to do with the original gap, $5.0J$. To explain the occurrence of an ESR line, we now consider the *global* single-ion anisotropy. The spectrum then acquires

*) The degeneracy of the low-lying triplets is lifted with respect to the exact solution, because discarding the quartic terms in the operators a , a^\dagger in the Hamiltonian has broken the total spin symmetry.

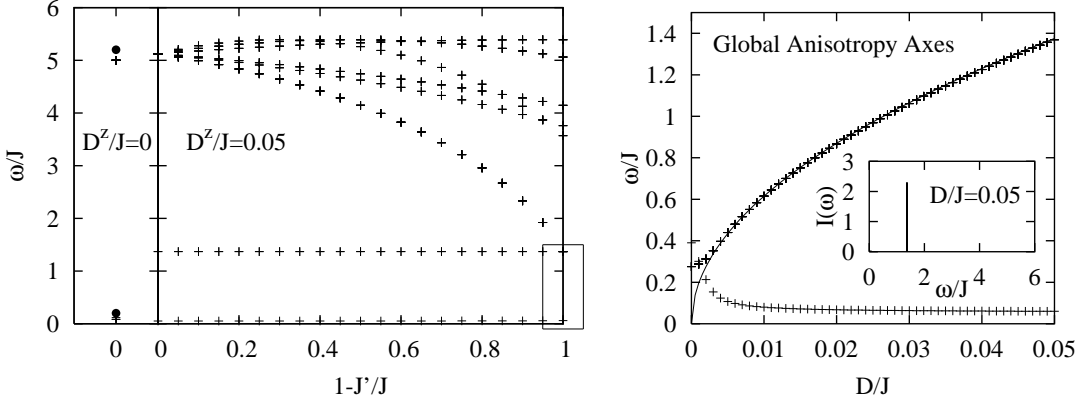


Fig. 4. Left: Low-energy modes vs. model parameter J'/J , where J' corresponds to coupling all the spins of a given sublattice to all the spins of another sublattice, for $D^z/J = 0; 0.05$. Comparison is given with the exact triplet energies of the fully connected model (solid black circles, $J' = J$, $D^z/J = 0$). The spectrum of the fully connected model¹⁴⁾ ($J' = J$) is different from that of the nearest neighbor Heisenberg model ($J' = 0$). Right: Two lowest energy modes vs. anisotropy D/J for the nearest-neighbor model ($J' = 0$) (note the scale: only the low frequency range of the left fig. is shown [corresponding to the box]). The second energy is very close to the \sqrt{D} behavior (solid line) of the classical antiferromagnetic resonance. Magnetic-dipole ESR intensities of the modes are given in the inset.

a resonance frequency that scales as $\sqrt{D/J}$ for D/J larger than about 0.003 (Fig. 4, right). The prefactor is numerically close to S^2 , $\omega = (2.48)^2\sqrt{D/J}$. This is similar to the *antiferromagnetic resonance* of the ordered antiferromagnets with single-ion anisotropy. For instance, for the infinite triangular lattice, we have $\omega = 3\sqrt{2D/J}$. When we suppress the Lagrange multipliers in the present system (which means that we restore the symmetry breaking of the Néel state), the frequency of the mode is almost unchanged provided $D/J \gtrsim 0.003$. Note that the Lagrange multipliers are still important in the present context to find the tower of states and at very small D ; but if one wants to calculate only the *frequency* of the antiferromagnetic resonance, one can consider the broken-symmetry state as being a good approximation. Nonetheless, to calculate the ESR intensity of a magnetic-dipole process,

$$I^\alpha(\omega) = \sum_e |\langle 0 | \sum_i S_i^\alpha | e \rangle|^2 \delta(\omega - \omega_e), \quad (3.6)$$

it is necessary to calculate not only the eigenvalues but also all the eigenvectors. That forces us to introduce proper Lagrange multipliers to avoid the singular transformation by suppressing the Goldstone modes. This calculation shows that the intensity is mainly in the *antiferromagnetic resonance* (and not in the other modes, in particular not in the higher energy modes) as shown in the inset of Fig. 4, right. The lowest energy mode also has an intensity, but it is much smaller. At this stage, it seems that everything is consistent with the recent ESR experiments where a single peak has been observed.¹³⁾ This may be an indication that the ground state of the system has indeed strong *coplanar* 120° short-range correlations as we have shown. We will, however, consider now a more realistic model that leads to a more

complicated excitation spectrum with additional peaks reflecting the *tangential* 120° correlations.

3.3. Model with Local Anisotropy Axes

We now consider a more realistic model where the vectors associated with D vary from site to site (model 2). We argue that the simple spectrum found in the previous section becomes more complicated and many ESR lines should be visible. Starting now from the mean-field ground state of Fig. 1 right, we calculate the correlations when the quantum fluctuations are added. In Fig. 5, we show the distribution of scalar products $\langle \mathbf{S}_i \cdot \mathbf{S}_j \rangle$. For the nearest neighbors, they are almost identical to the classical scalar products, thus confirming the very strong correlations between the nearest neighbors (Fig. 5, left). For neighbors that belong to opposite sides of the sphere, the correlations have been reduced and the distribution has a large peak at zero, but is still broad (Fig. 5, right). For this model, correlations between far neighbors are weaker.

Concerning the thermodynamic quantities, the specific heat, for instance, is very similar to that of the simpler model with global anisotropy, and weakly dependent upon the strength of the anisotropy (Fig. 3). In particular we note that it would not be possible to distinguish between the different models on the basis of the specific heat only. However, the ESR spectrum shows different features. We have calculated the frequencies and their intensities (Fig. 6). All the frequencies get some intensity. There is indeed no selection rule such as $\Delta q = 0$ in the present case where all sites have a different classical magnetization. This is in contrast to the classical 3-sublattice state previously discussed where the correlations are simpler. Experimentally it is plausible that the states are mixed and appear as a broader line (see the convolution with Gaussian functions in Fig. 6).

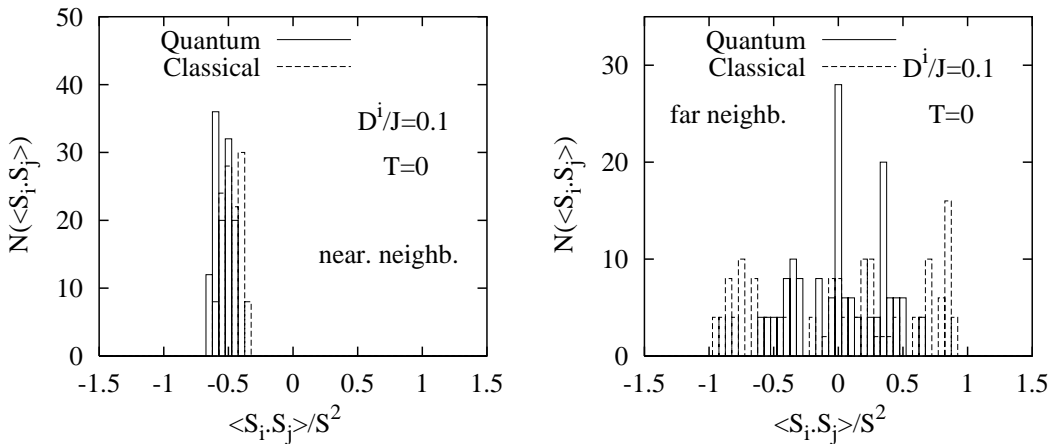


Fig. 5. Number of bonds with a given value of the correlation function for the nearest neighbors (left) and the furthest-away bonds (right). Local anisotropy axis. For definition of “quantum” and “classical”, see fig. caption 2.

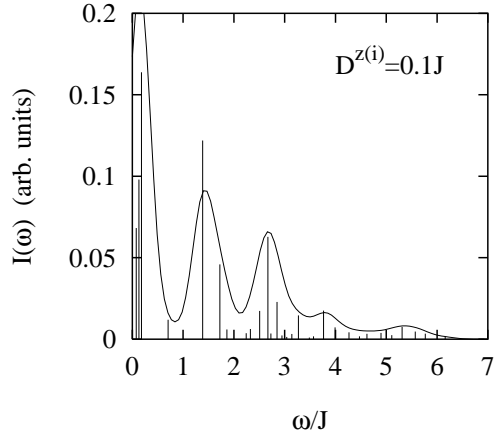


Fig. 6. ESR intensity of the modes of energy ω (spikes) for the model with *local* anisotropies. The curve is a convolution of the spikes with Gaussian functions.

§4. Conclusion

We have addressed the role of the quantum fluctuations and the anisotropy in a complex molecular compound, $\text{Mo}_{72}\text{Fe}_{30}$. First, we note that the specific heat at low temperatures is strongly suppressed by quantum effects and weakly dependent upon the strength of the anisotropy, contrary to classical approaches.¹²⁾

The ground state depends, however, upon the anisotropy we choose. We have described the short-range correlations in the ground state and shown that the correlation length at zero-temperature is of the order of the size of the molecule. A local anisotropy which respects the geometry of the sphere favors *tangential* short-range correlations (as in Fig. 1, right), whereas global anisotropy axes or, possibly, fluctuations would favor *coplanar* correlations (Fig. 1, left). The nature of the correlations could be directly tested by elastic neutron scattering.

Moreover, we have shown that the excitation spectrum exhibits different features depending on the nature of the ground state. When the spins are coplanar, the spectrum consists of an *antiferromagnetic resonance* (as in classical systems) with a \sqrt{DJ} behavior for D not too small, separated from higher magnon states by a sizeable gap. Magnetic-dipole ESR transitions are found to be allowed from the ground state to the antiferromagnetic resonance only. The other states should be visible in inelastic neutron scattering, for instance.

For a ground state with tangential correlations, the excitation spectrum is more complex and a quasi continuum of magnon states is found at low energy (fig. 6). In this case, because all the sites have different spin directions (and the symmetries relating different sites are completely broken), there is no selection rule for magnetic-dipole transitions: all the modes acquire some intensity. Combined with other relaxational mechanisms, the overall effect would be to give a very broad ESR signal, as indicated in the figure. Unusually large broadening seems to be observed experimentally.¹³⁾ It could be taken as an indication that the ground state has *tan-*

gential short-range correlations rather than *coplanar*, although, strictly speaking, the comparison needs to be done at finite fields.

A general feature of finite-size systems is the tower of states at very low energy. Takahashi's method provides a way to go beyond the scaling limit result for calculating the energy of the magnon modes of the tower of states, and we have given their energy. It would be interesting to observe these modes, which would explain the slow dynamics of these systems.

Acknowledgments

It is a pleasure to thank Prof. H. Nojiri who has stimulated this work and who has provided us with his experimental data prior to publication.

References

- 1) G. Misguich, C. Lhuillier, Chapter to appear in the book "Frustrated spin systems", edited by H. T. Diep, World-Scientific (2003), cond-mat/0310405.
- 2) A. Müller, M. Luban, C. Schroeder, R. Modler, P. Kögerler, M. Axenovich, J. Schnack, P. Canfield, S. Bud'ko, and N. Harrison, *ChemPhysChem* 2, 517 (2001).
- 3) S. I. Kiselev, J. C. Sankey, I. N. Krivorotov, N. C. Emley, R. J. Schoelkopf, R. A. Buhrman and D. C. Ralph, *Nature* **425**, 380 (2003).
- 4) P. W. Anderson, *Phys. Rev.* **86**, 694 (1952).
- 5) H. Kawamura and S. Miyashita, *J. Phys. Soc. Jpn.* **54**, 4530 (1985).
- 6) M. E. Zhitomirsky, *Phys. Rev. Lett.* **88**, 057204 (2002).
- 7) C. Schroeder, H. Nojiri, J. Schnack, P. Hage, M. Luban, and P. Koegerler, cond-mat/0405405, submitted to *Phys. Rev. Lett.*
- 8) B. Barbara, L. Thomas, F. Lioni, I. Chiorescu, A. Sulpice, *J. Magn. Magn. Mater.* **200**, 167 (1999).
- 9) J. Schnack, H.-J. Schmidt, J. Richter, and J. Schulenburg, *Eur. Phys. J. B* **24**, 475 (2001).
- 10) M. E. Zhitomirsky, and H. Tsunetsugu, *Phys. Rev. B* **70**, 100403 (2004).
- 11) M. Axenovich and M. Luban, *Phys. Rev. B* **63**, 100407 (R) (2001).
- 12) M. Hasegawa and H. Shiba, *J. Phys. Soc. Jpn.* **73**, 2543 (2004).
- 13) H. Nojiri : private communication.
- 14) J. Schnack, M. Luban, and R. Modler, *Europhys. Lett.* **56** (6), 863 (2001).
- 15) M. Exler and J. Schnack, *Phys. Rev. B* **67**, 094440 (2003).
- 16) T. Sakai, O. Cépas, and T. Ziman, *J. Phys. Soc. Jpn.* **69**, 3521 (2000).
- 17) O. Cépas, K. Kakurai, L. P. Regnault, J. P. Boucher, T. Ziman, N. Aso, M. Nishi, H. Kageyama, and Y. Ueda, *Phys. Rev. Lett.* **87**, 167205 (2001); O. Cépas and T. Ziman, *Phys. Rev. B* **70**, 024404 (2004).
- 18) M. Takahashi, *Prog. Theor. Phys. Suppl.* **87**, 233 (1986).
- 19) M. Takahashi, *Phys. Rev. B* **40**, 2494 (1989).
- 20) M. Luban, *J. Magn. Magn. Mater.* **272-276**, e635 (2004).
- 21) L. R. Walker, in *Magnetism*, Vol. 1, edited by G.T. Rado and H. Suhl, Academic Press (1963).
- 22) R. M. White, M. Sparks and I. Ortenburger, *Phys. Rev.* **139**, A450 (1965).
- 23) Y. Watabe, T. Suzuki and Y. Natsume, *Phys. Rev. B* **52**, 3400 (1995).
- 24) A. G. Del Maestro and M. J. P. Gingras, *J. Phys. Condens. Matt.* **16**, 3339 (2004).
- 25) A. E. Trumper, L. Capriotti and S. Sorella, *Phys. Rev. B* **61**, 11529 (2000).
- 26) B. Bernu, C. Lhuillier, and L. Pierre, *Phys. Rev. Lett.* **69**, 2590-2593 (1992). B. Bernu, P. Lecheminant, C. Lhuillier, and L. Pierre, *Phys. Rev. B* **50**, 10048 (1994).
- 27) J. E. Hirsch and S. Tang, *Phys. Rev. B* **40**, 4769 (1989).
- 28) E. Rastelli and A. Tassi, *Phys. Lett.* **48 A**, 119 (1974).
- 29) G. S. Rushbrooke, G. A. Baker, and P. J. Wood, in *Phase Transitions and Critical Phenomena*, Vol. 3, Edited by C. Domb and M.S. Green (Academic Press, London).
- 30) O. Waldmann, *Phys. Rev. B* **65**, 024424 (2001).